A Gentle Sedimentation Process for Size-Selecting Porous Silicon Microparticles to Be Used for Drug Delivery Via Fine Gauge Needle Administration

Nekovic, Elida; Storey, Catherine J.; Kaplan, Andre; Theis, Wolfgang; Canham, Leigh T.

DOI:
10.1007/s12633-020-00895-3

Silicon
https://doi.org/10.1007/s12633-020-00895-3

ORIGINAL PAPER

A Gentle Sedimentation Process for Size-Selecting Porous Silicon Microparticles to Be Used for Drug Delivery Via Fine Gauge Needle Administration

Elida Nekovic[1] · Catherine J. Storey[1] · Andre Kaplan[1] · Wolfgang Theis[1] · Leigh T. Canham[1]

Received: 30 September 2020 / Accepted: 10 December 2020

Abstract
Biodegradable porous silicon (pSi) particles are under development for drug delivery applications. The optimum particle size very much depends on medical use, and microparticles can outperform nanoparticles in specific instances. Here we demonstrate the ability of sedimentation to size-select ultrasmall (1–10 μm) nanoporous microparticles in common solvents. Size tunability is quantified for 1–24 h of sedimentation. Experimental values of settling times in ethanol and water are compared to those calculated using Stokes' Law. Differences can arise due to particle agglomeration, internal gas generation and incomplete wetting. Air-dried and supercritically-dried pSi powders are shown to have, for example, their median diameter d (0.5) particle sizes reduced from 13 to 1 μm and from 20 to 3 μm, using sedimentation times of 6 and 2 h respectively. Such filtered microparticles also have much narrower size distributions and are hence suitable for administration in 27 gauge microneedles, commonly used in intravitreal drug delivery.

Keywords Size selection sedimentation · Stokes' Law · Porous silicon microparticles · Silicon aerocrystal · Intravitreal injection

1 Introduction

Mesoporous materials as vehicles for drug delivery within the body are currently the focus of rigorous research [1, 2]. They can be administered orally, via intravenous injection, or directly into targeted tissues [3]. Mesoporous silicon can provide a very high drug payload matrix [4] which is biocompatible, biodegradable and of tunable pore size for different drug molecules and variable release rates [5].

Porous silicon particulates for drug delivery can be divided into two size categories: microparticles and nanoparticles. The choice of particle category is highly dependent on the application and naturally, there are advantages and disadvantages to both [6]. Nanoparticles, with higher comparative surface areas and shorter diffusion distances, experience faster dissolution and faster drug release, often over a matter of hours [7]. These are well suited to oral delivery applications, wherein drug delivery is determined by the time frame of its passage through the digestive tract. Such ultrasmall particles also remain mobile, even after parenteral delivery and hence are typically suited to systemic treatments, whilst their ultrasmall size enables them to enter cells by endocytosis and work within [6]. In contrast, microparticles can offer higher internal drug payloads and slower release rates [8]. Their larger size also renders the particles relatively immobile at the site of delivery. Porous silicon microparticles are thus highly suited to the specific targeting of organs such as the liver or pancreas, where clinical trials for brachytherapy are on-going [9, 10]. Another opportunity for biodegradable microparticles is retinal conditions [11] where slow-release formulations are urgently needed to reduce the frequency of intravitreal injections required, thereby significantly enhancing patient comfort. In this study, we have focused on achieving very small microparticles, rather than nanoparticles.

The fabrication process is another important consideration to tailor pore size for the loading of specific molecules in a top-down approach, using highly tunable electrochemical anodisation [12]. Comminution processes such as ball milling or sonication can then be used to produce particles within a chosen size range [13].

✉ Elida Nekovic
exn694@student.bham.ac.uk; exn694@alumni.bham.ac.uk

[1] Nanoscale Physics Research Laboratory, School of Physics & Astronomy, University of Birmingham, Birmingham, Edgbaston B15 2TT, UK

For drug delivery via needle administration, size selection of the ensuing microparticles is an important step. A narrow size distribution with minimal outliers will help prevent needles from clogging [14], whilst finer gauge needles improve patient comfort. Needle gauges of 25G or 27G are considered a good compromise of injectability and comfort [15, 16]. A 27G needle has an internal diameter of only about 200 μm and it is recommended that all particles should be below 20-μm diameter to avoid needle blockage through particle agglomeration [15, 16].

In order to ensure a tight size distribution, various methods can be employed. For nanoparticles, sonication followed by centrifugation is a popular method but is often time-consuming and requires additional processing steps [17, 18]. Alternatively, for microparticles, filtering or sieving using metal sieves, can enable the selection of particles below 20 μm. However, the process can impart undesirable metal contamination [12] since it requires violent agitation of powder, which is also likely to cause damage.

Alternatively, we show here, using sedimentation, this gentle size selection procedure can be achieved in a suitable time frame with resulting narrow size distributions. If anodisation-sonication-sedimentation-drug loading is sequentially used, then small ultrahigh porosity microparticles ("aerocrystals") can completely avoid drying induced structural damage, prior to drug loading. In addition, we show here that in contrast repeated drying steps during manufacture can significantly lower pore volume and thereby drug payloads.

Sedimentation has hardly been exploited at all with porous silicon and prior works have not studied it quantitatively [19]. Here, we use Stokes' Law calculations to investigate the likely settling velocities for silicon particles of varying porosity and size in two common solvents: water for hydrophilic particles and ethanol for hydrophobic particles. We then experimentally investigate the porous silicon microparticle size range for which sedimentation can provide a practical processing tool.

Prior quantitative sedimentation studies of some other materials, together with this study, are listed in Table 1. We see that submicron particles, even when non-porous, require very long settling times, whilst quite small microparticles have moderate settling times that are strongly dependent on particle size and density.

2 Experimental Methods

2.1 Porous Silicon Microparticle Preparation

Porous silicon membranes were first prepared by electrochemical anodisation of heavily boron-doped crystalline silicon wafers (0.005–0.02 Ωcm). These six-inch diameter wafers were anodised in a double cell by applying a current density of 130 $mAcm^{-2}$ for 46 min, whilst circulating an electrolyte mix of 1:1 40 wt% hydrofluoric acid and ethanol. An increased current density of 165 $mAcm^{-2}$ was subsequently applied at the end of this cycle for a few seconds, to facilitate electropolishing and detachment of the porous silicon membrane. Lower porosity membranes (sample UoB 101 49%) were collected and rinsed in ethanol before drying in the air on a hotplate at 60 °C for 3 h. Alternatively, for the preservation of high porosity membranes (sample UoB99 85%) supercritical drying (SCD) using a Quorum Technologies Limited K850 critical point drier was used [4, 23, 24]. Ball milling was then utilized to rapidly create large quantities of microparticles by using a Fritsch planetary ball miller at 300 rpm for only 1 min. Here a 500 ml zirconium oxide grinding bowl, together with 120 individual 10 mm diameter zirconium oxide grinding balls, were used to generate batches of porous silicon powder up to approximately 7 g. Hydrophobic microparticles were created by anodisation, rinsing, drying and milling but could be rendered hydrophilic by subsequent high-temperature oxidation for 16 h at 700 °C in diluted oxygen using a ThermoScientific rotary furnace.

2.2 Size Selection Sedimentation Trials

Five - 1 g hydrophilic samples of air-dried, ball-milled and oxidised mesoporous silicon powder of 48.4% porosity were individually mixed with 20 ml of deionized water in separate glass vials and thoroughly vortex mixed. They were subsequently subjected to sedimentation in deionized water at room temperature for different time periods from 1 to 24 h in a 5 cm

Table 1 Particle size range, settling velocity and settling time for different types of particles from prior sedimentation studies and the current study

Reference	Type of particle Density (g/cm^3)	Particle size range (μm)	Settling velocity (cm/h)	Settling times utilized	Sedimentation solvent
Vida-Simiti 2012 Ref. [20]	Solid Nickel 8.90	2–90	5000–72,463	5–75 s	Water
Giddings 1991 Ref. [21]	Porous silica 1.48–1.67 (dry)	2.31–7.48	1270–2571	2.08–4.49 min	Water
This study	*Porous silicon 1.02–1.67 (immersed)*	1–70	*0.04–5*	*1–24 h*	*Water, Ethanol*
Philipse 1990 Ref. [22]	Solid Silica 1.80	0.6–0.72	0.04–0.09 & 6.3	100–200 h	Water, Ethanol

high liquid column. After the allocated times, the supernatant from each vial was carefully and completely drawn off using a plastic Pasteur pipette and the solvent was removed at 60 °C in a Genlab drying cabinet until no further weight reduction was observed. The final dry weight was recorded and thereby the overall pSi supernatant yield calculated (dried supernatant weight/ original pSi weight × 100%). A similar 2-h sedimentation procedure in ethanol was applied to 85% porosity supercritically-dried pSi flakes, that had been subsequently ball-milled in order to form a suspension of hydrophobic microparticles. Particle sizing of the supernatants collected after different sedimentation times were performed (see below).

2.3 Characterisation

- Gas Adsorption Analysis – Nitrogen gas adsorption analysis using a Micromeritics Tristar 3020 was used to establish pore characteristics including; surface area, using the Brunauer-Emmett-Teller method (BET) applied to the adsorption branch of the isotherm; pore volume, using the Barrett-Joyner-Halender (BJH) adsorption method; and pore diameter using the adsorption average.
- Particle Sizing – Samples were thoroughly vortex mixed prior to particle sizing. A Malvern Mastersizer 2000, employing laser diffraction at 466 nm, was then used to perform an analysis of particle size distributions within each sample, whilst dispersed in deionised water with the assistance of 5 wt% Igepal.

3 Results

3.1 Stokes' Law Calculations of Sedimentation Velocities

The settling times for idealized spherical particles in a liquid were calculated (see Table 2) using Stokes' Law equation $t = \frac{18\eta s_d}{d^2 g\left(\rho_p - \rho_f\right)}$ [25], where: d is the diameter of the particle; ρ_p is the mass density of the particle; ρ_f is the mass density of the fluid; η is the dynamic viscosity of the fluid; g is gravitational acceleration, and s_d is the sedimentation distance. A key assumption made for porous particles was that the solvent supporting the particles completely wetted each particle, removing entrapped air. Particle densities used were thus: 2.33 g/cm^3 for solid silicon; 1.18 g/cm^3 for SCD pSi in water, 1.02 g/cm^3 for SCD pSi in ethanol,. 1.67 g/cm^3 for oxidised pSi in water and 1.57 g/cm^3 for oxidised pSi in ethanol. Fluid densities used were: 997 kg/m^3 for water and 789 kg/m^3 for ethanol, respectively. Viscosity parameters (at room temperature) used were: $8.90 \cdot 10^{-4}$ Pas for water and $9.83 \cdot 10^{-4}$ Pas for ethanol, respectively.

3.2 Materials Used in Drying, Storage and Sedimentation Experiments

Gas adsorption analysis data of supercritically-dried samples UoB 99 and 102, together with air-dried sample UoB 101 used in drying, storage and sedimentation experiments are shown in Table 3.

3.3 Effects of Drying and Humidity Variations during Storage of Silicon Aerocrystals

Sedimentation in solvents, unlike metal sieve filtration, is a technique of size selection that can be used without the need to dry porous silicon particles created by wet electrochemical etching. We therefore first conducted experiments to explore just how damaging air drying followed by storage in ambient air of varying humidity might be for very highly porous large microparticles. Large reductions in porosity accompanying the use of dry size classification processes would underpin the need for wet processing alone, before drug loading, to maximise payloads [4].

Lengthy storage in the air of varying humidity can cause water adsorption-desorption induced stresses, influencing the pore characteristics and structural integrity of SCD pSi material. During fabrication and processing, it is also often necessary to repeatedly soak the pSi (in a solvent such as methanol) and then re-dry, for example after anodisation and then again after a wet surface treatment. Repeated exposure of high porosity silicon microparticles to a methanol solution was hence undertaken to ascertain what degree of damage might be sustained in such circumstances. A methanol-water mixture rather than pure water was used to wet the very high porosity hydrophobic microparticles. To ensure no damage was caused prior to these trials, the pSi material had been supercritically dried, a technique known to preserve high porosities [4]. Gas adsorption analysis was carried out to calculate the initial pore volume & pore diameter of a 100 mg SCD pSi sample. The sample was then re-wetted in a 20 ml solution of 50:50 MeOH: DI water for 5 min before air drying on a hotplate at 60 °C for 3 h. The sample was reprocessed three more times, using the same soak/dry cycle and gas adsorption analysis was carried out after each cycle Results are shown in Fig. 1.

3.4 Size Distribution Versus Sedimentation Time for Oxidised Porous Silicon Microparticles in Water

Figure 2 illustrates the visual appearance of a sample UoB 101 suspensions after sedimentation times varying from 1 to 24 h. Table 4 and Fig. 3 quantify the size distributions and yields of the supernatants collected.

Table 2 Stokes' Law calculations of settling times for solid and porous silicon microparticles in water and ethanol. (maximum sedimentation distance $s_d = 5$ cm as shown in Fig. 2)

Material	Particle Diameter (microns)	Stokes' Law Settling Time for water & $s_d = 5$ cm	Stokes' Law Settling Time for ethanol & $s_d = 5$ cm
Solid silicon (2.33 g/cm^3)	100	6.1 s	5.8 s
	50	24.5 s	23.4 s
	10	10.2 mins	9.7 mins
	1	17.1 h	16.3 h
	0.1	70.8 days	67.8 days
Oxidised porous silicon	100	11.9 s	11.4 s
In water 1.67 g/cm^3. In ethanol 1.57 g/cm^3	50	0.8 mins	0.7 mins
	10	19.9 mins	19.2 mins
	1	1.4 days	1.3 days
SCD Porous Silicon	100	44.1 s	39.1 s
In water 1.18 g/cm^3. In ethanol 1.02 g/cm^3	50	2.9 mins	2.6 mins
	10	1.2 h	1.1 h
	1	5.1 days	4.5 days

Table 3 Pore volume/porosity, surface area and mean pore size values for supercritically-dried (SCD) sample UoB 102, air-dried (AD) pSi sample UoB 101 and supercritically-dried pSi sample UoB 99, before and after ball milling (BM)

Sample code	Pore volume (ml/g)	Porosity from pore volume (%)	Surface area (m^2/g)	Mean pore size (nm)
UoB 102 (SCD)	3.39	88.70	506	26.87
UoB 101 (AD)	0.40	48.40	142	10.50
UoB 99 (SCD)	2.40	84.90	400	22.90
UoB 99 (SCD + BM)	1.21	74.90	251	19.30

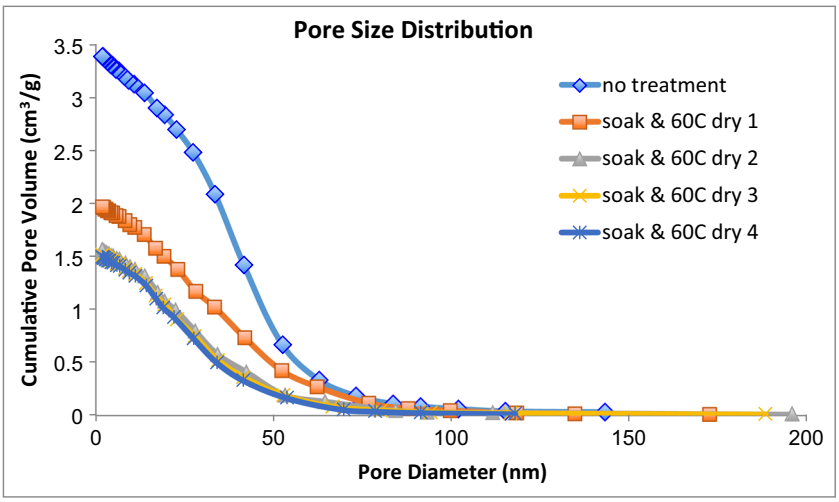

Fig. 1 Pore volume/pore size distribution in SCD pSi (Sample UoB 102) during repeated capillary condensation/ evaporation (0–4 soak/dry cycles)

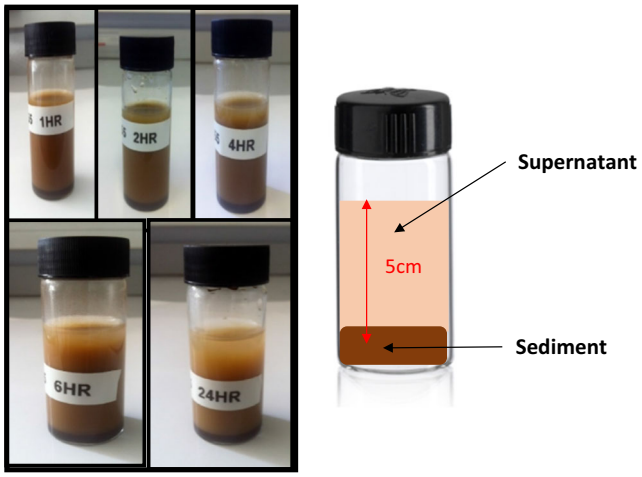

Fig. 2 Optical image of individual UoB 101 samples during different sedimentation times in water

3.5 Size Distribution Change by Sedimentation for Supercritically-Dried Porous Silicon in Ethanol

Table 5 and Fig. 4 present the particle size distributions data after 2-h sedimentation.

4 Discussion

The results of experiment 1 (Section 3.3) showed that both air drying and storage in ambient air can lower pore volumes, especially if the humidity of the air varies with time, leading to repeated wetting-drying cycles. It is clear that significant porosity degradation can accompany porous silicon fabrication sequences that involve more than one drying step. It is considered that the majority of damage is caused by the most fragile pore walls collapsing due to the surface tension and capillary forces exerted by the liquid during evaporation in the first two soak/dry cycles (Fig. 1). The remaining porous infrastructure is more robust, with limited further deterioration taking place on consecutive soak/dry cycles.

Table 4 *Particle sizing and yield of pSi for air-dried sample UoB 101 after sedimentation over varying times.* The d value represents particle diameter in microns and the values are shown in the table refer to the cumulative volume of particles below this size as a percentile

Sedimentation time (h)	Particle size (μm) d (0.1)	Particle size (μm) d (0.5)	Particle size (μm) d (0.9)	The yield of pSi particles (%)
0 (control sample)	1.61	13.39	34.02	N/A
1	0.66	2.47	9.90	13.22
2	0.60	1.70	3.45	7.59
4	0.55	1.29	2.48	4.99
6	0.54	1.12	2.07	2.57
24	0.25	0.59	1.32	0.35

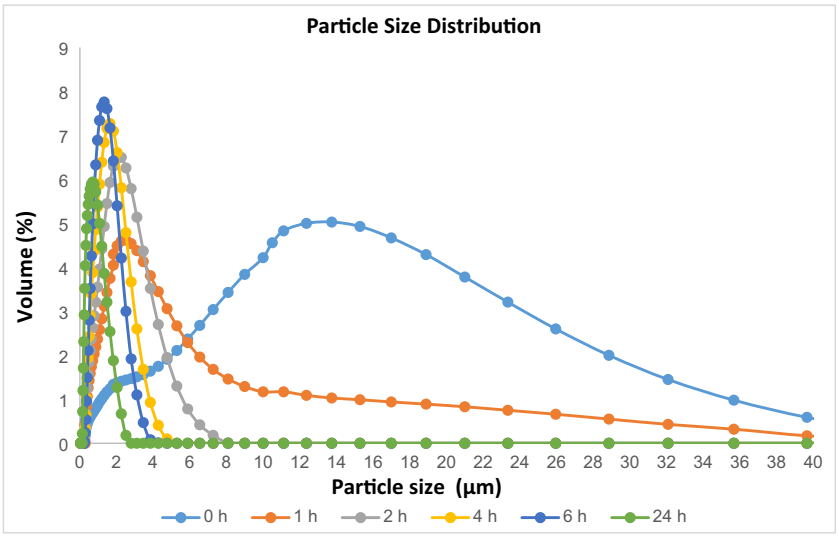

Fig. 3 Particle Size Distribution of air-dried sample UoB 101 for sedimentation times from 0 to 24 h

Table 5 Particle sizing and yield of pSi data for supercritically-dried sample UoB 99 are presented in the table below

Sample details	Particle size (μm) d (0.1)	Particle size (μm) d (0.5)	Particle size (μm) d (0.9)	The yield of pSi particles (%)
SCD + BM	2.00	19.71	68.49	N/A
SCD + BM + 2 h sedimentation	0.79	2.91	8.98	11.38

Experiment 2 (Section 3.4) aimed to quantify the size tunability of the sedimentation technique for porous silicon particles and common solvents such as water (Fig. 2). Particle size distribution data (Fig. 3 and Table 4) shows a consistent trend for narrowing spread and smaller particles held in suspension with increasing time. After 1 h of sedimentation, the peak particle size of the oxidised porous silicon sample (UoB 101) is approximately 2.2 μm, but a significant volume of particles above 10 μm remain in suspension at this stage. By 6 h a much tighter size distribution is apparent with a peak particle size of 1.5 μm whilst particles above 4 μm have now sedimented out. This is significantly *faster* than Stokes' Law (Table 2) predicts whereby it is calculated that 4 μm particles would take 27 h to settle. The discrepancy can be attributed to particle agglomeration, as suggested by prior sedimentation studies, summarized in Table 1, attributing it to a tendency of small particles to diminish their higher surface energies. At 24 h, the trend in experimental data continues with peak particle size and upper particle size in the supernatant being 1 μm & 3 μm respectively.

Experiment 3 (Section 3.5) explored the use of sedimentation for very low-density silicon aerocrystals. Supercritically-dried high porosity pSi is the most mechanically fragile porous silicon nanostructures and benefits most from gentle processing techniques like sedimentation. Following a 2 h sedimentation period, the peak size of particles in the supernatant was 3.5 μm with all particles above 50 μm having settled (Fig. 4). Stokes' equation predicts that 50 μm particles in ethanol should need only 2.6 mins to settle whilst 10 μm particles need 1.1 h and 1um particles need 4.5 days. It is evident (from Fig. 4) that there are still substantial numbers of 10-μm particles that have not sedimented after 2 h. This is *slower* than predicted by Stokes' Law and might arise from a number of factors, such as internal hydrogen gas generation due to oxidation, incomplete solvent wetting of the silicon aerocrystal particles or their partial fragmentation due to dissolution in the solvent. Further detailed studies are needed to evaluate which of these is dominant.

In summary, settling time depends on the density and viscosity of the solvent, but more significantly on the particle size and particle density, which follows an inverse relationship (Table 2). It is proposed that for sedimentation in the water, the particle agglomeration appears more pronounced than in ethanol. Short sedimentation times of 1–2 h in both water and ethanol can be used to extract 1–10 μm porous silicon particles with yields above 10%. Settling times and yields in water are affected by particle agglomeration, thus the process might benefit from surface modifications to increase particle surface charge.

We have previously shown that even longer ethanol storage does not cause any further change to the pore volume and surface area of the material [4]. Therefore, sedimentation is considered as a gentle procedure for narrowing the particle size distribution below a certain value.

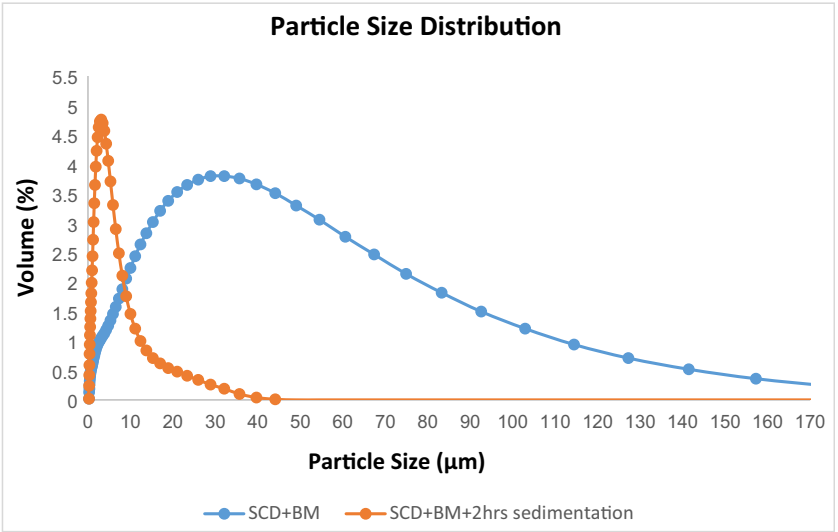

Fig. 4 The particle size distribution of SCD material UoB 99 before and after 2 h sedimentation

5 Conclusion

We demonstrated the ability of sedimentation as a processing tool for size selectivity of microparticles below 10 μm in solvents such as deionized water and ethanol. Prior sedimentation studies on porous silicon have not performed a quantitative analysis. Accordingly, using Stokes' Law we calculated settling times for porous silicon particles of different densities. We found that experimentally, particles are settling significantly faster than predicted for higher density (low porosity) oxidised pSi microparticles in water and slightly slower for lower density (high porosity) supercritically-dried pSi microparticles in ethanol.

Using sedimentation, we ensured a very tight microparticle size distribution when using 49% porosity oxidised pSi material after only 2 h of processing and for this material achieved particle sizes are therefore suitable for fine-gauge needle administration. However, using SCD pSi material of 85% porosity over the same 2 h period, the upper particle size approached 50 μm. Such outliers, whilst below the internal diameter of a 27G needle, are still too large to guarantee prevention of needle clogging if an aspect ratio of 0.1 is applied (relating to a particle size below 20 μm [15]). It is believed that longer sedimentation periods using this material are capable of reducing the particle size maximum to within acceptable limits and is currently under investigation.

We confirmed here that repeated drying steps during manufacturing can significantly lower pore volume and thereby drug payloads. Contrary to sedimentation, lengthy storage in the air can cause significant degradation of porosity. We claim that the following order of fabrication/processing steps: anodisation-sonication-sedimentation-drug loading enables complete avoidance of drying and humid air storage induced structural damage, before drug loading.

Acknowledgements EN would like to thank the School of Physics & Astronomy at the University of Birmingham for funding her doctoral research.

Author Contributions EN, CJS and LTC designed the studies; EN conducted the Stokes Law calculations; EN and CJS performed the experimental work; AK,WT and LTC managed the project. All authors contributed to writing and approving the final version of the paper.

Funding This research was funded by the School of Physics & Astronomy, University of Birmingham.

Data Availability Raw data and material are available on request.

Compliance with Ethical Standards

The authors declare that they have no known competing financial interest or personal relationships that could have appeared to influence the work reported in this paper.

Consent to Participate All authors voluntarily agree to participate in this research study.

Consent for Publication All authors give the permission to the Journal to publish this research study.

References

1. Santos HA, Salonen J, Bimbo LM, Lehto V-P, Peltonen L, Hirvonen J (2011). Mesoporous materials as controlled drug delivery formulations. J Drug Del Sci Technol 2-1(2):139–155
2. Kennedy E, Canham L (2016). Mesoporous biomaterials: a lexicon and structured Bibliography of Reviews. HA Santos. Open Mater Sci 3:1–14
3. Salonen J, Kaukonen AM, Hirvonen J, Lehto VP (2008). Mesoporous silicon in drug delivery applications. J Pharm Sci 97: 632–653
4. Nekovic E, Storey CJ, Kaplan A, Theis W, Canham LT (2020). Communication—supercritically-dried membranes and powders of >90% porosity silicon with pore volumes exceeding 4 cm^3g-1. ECS J Sol State Sci Technol 9:024016
5. Li W, Liu Z, Fontana F, Ding Y, Liu D, Hirvonen JT, Santos HA (2018). Tailoring porous silicon for biomedical applications: from drug delivery to cancer immunotherapy. Adv Mater 30:24
6. Kohane DS (2007). Microparticles and nanoparticles for drug delivery. Biotechnol Bioeng 96:203–209
7. Lee JH, Yeo Y (2015) Controlled drug release from pharmaceutical nanocarriers. Chem Eng Sci 125:75–84
8. Tzur-Balter A, Rubinski A, Segal E (2013). Designing porous silicon-based microparticles as carriers for controlled delivery of mitoxantrone dihydrochloride. J Mater Res 28(2):231–239
9. Canham LT (2014) in Porous Silicon for Biomedical Applications, Edited by H. Santos, Woodhead Publishing, Series in Biomaterials No 88, pp 3–20
10. Goh AS, Chung AY, Lo RH, Lau TN, Yu SW, Chng M, Satchithanantham S, Loong SL, Ng DC, Lim BC, Connor S, Chow PK (2007). A novel approach to brachytherapy in hepatocellular carcinoma using a phosphorus 32brachytherapy delivery device – a first in man study. Intnl J Radiation Oncol Biol Phys 67(3):786–792
11. Warther D, Xiao Y, Li F, Wang Y, Huffman K, Freeman WR, Sailor M, Cheng L (2018) Porous silicon based intravitreal platform for dual-drug loading and controlled release towards synergistic therapy. Drug Deliv 25(1):1537–1545
12. Loni A (2018) In: Canham L (ed) Handbook of Porous Silicon. Springer, Cham, pp 1051–1061
13. Storey CJ, Nekovic E, Kaplan A, Theis W, Canham LT (2020) Preserving surface area and porosity during fabrication of silicon aerocrystal particles from anodized wafers. J Porous Mater 30(4):1–6

14. Puthli S, Vavia PR (2009) Stability Studies of Microparticulate System with Piroxicam as Model Drug. AAPS PharmSciTech 10(3):872–880
15. Miller MA, Engstrom JD, Ludher BS, Johnston KP (2010) Low Viscosity Highly Concentrated Injectable Nonaqueous Suspensions of Lysozyme Microparticles. Langmuir 26(2):1067–1074
16. Whitaker MA, Langston P, Naylon A, Azzopardi BJ, Howdle SM (2011) Particle size and shape effects in medical syringe needles: experiments and simulations for polymer microparticle injection. J Mater Sci Mater Med 22:1975–1983
17. Hon NK, Shaposhnik Z, Diebold ED, Tamanoi F, Jalali B, Biomed J (2012) Tailoring the biodegradability of porous silicon nanoparticles. Mater Res Part A 100A:3416–3421
18. Roberts DS, Estrada D, Yagi N, Anglin EJ, Chan NA, Sailor MJ (2017) Preparation of Photoluminescent Porous Silicon Nanoparticles by High-Pressure Microfluidization. Part Part Syst Charact 34:1600326
19. Litvinenko S, Alekseev S, Lysenko V, Venturello A, Geobaldo F, Gulina L, Kuznetsov G, Tolstoy V, Skryshevsky V, Garrone E, Barbier D (2010) Hydrogen production from nano-porous Si powder formed by stain etching. Int J Hydrog Energy 35:6773–6778
20. Vidi-Simiti IV, Jumate N, Thalmaier G, Sechel N, Moldovan V (2012). Measurement of particle density, porosity, and size distributions by sedimentation/steric field-flow fractionation: application to chromatographic supports. J. Porous Mater 19:21–27
21. Giddings JC, Moon MH (1991). Measurement of particle density, porosity, and size distributions by sedimentation/steric field-flow fractionation: application to chromatographic supports. Anal Chem 63:24
22. Philipse AP, Bonekamp BC, Veringa HJ (1990). Colloidal filtration and [simultaneous) sedimentation of alumina and silica suspensions: influence of aggregates. J Am Ceram Soc 73(9):2720–2727
23. Canham LT, Cullis AG, Pickering C, Dosser OD, Cox TI, Lynch TP (1994) Luminescent anodized silicon aerocrystal networks prepared by supercritical drying. Nature 368(6467):133–135
24. Loni A, Canham LT, Defforge T, Gautier G (2015). Supercritically-Dried Porous Silicon Powders with Surface Areas Exceeding 1000 m^2/g. ECS J Solid State Sci Technol 4(8):289–292
25. Sediq AS, Waasdorp SKD, Nejadnik MR, van Beers MMC, Meulenaar J, Verrijk R, Jiskoot W (2017) Determination of the Porosity of PLGA Microparticles by Tracking Their Sedimentation Velocity Using a Flow Imaging Microscope (FlowCAM). Pharm Res 34:1104–1114